The Journal of Experimental Biology 214, 1123-1130

doi:10.1242/jeb.043596

RESEARCH ARTICLE

Toe function and dynamic pressure distribution in ostrich locomotion

Nina Ursula Schaller[1,2,*], Kristiaan D'Août[3], Rikk Villa[2], Bernd Herkner[2] and Peter Aerts[3,4]

[1]University of Heidelberg, Department of Morphology/Ecology, INF 230, 69120 Heidelberg, Germany, [2]Senckenberg Research Institute, Senckenberganlage 25, 60325 Frankfurt/M. Germany, [3]University of Antwerp, Department of Biology, Functional Morphology, Universiteitsplein 1, 2610 Wilrijk, Belgium and [4]University of Ghent, Department of Movement and Sports Sciences, Watersportlaan 2, 9000 Ghent, Belgium

*Author for correspondence (nina.schaller@senckenberg.de)

Accepted 10 December 2010

SUMMARY

The ostrich is highly specialized in terrestrial locomotion and is the only extant bird that is both didactyl and exhibits a permanently elevated metatarsophalangeal joint. This extreme degree of digitigrady provides an excellent opportunity for the study of phalangeal adaptation towards fast, sustained bipedal locomotion. Data were gathered in a semi-natural setting with hand-raised, cooperative specimens. Dynamic pressure distribution, centre of pressure (CoP) trajectory and the positional inter-relationship of the toes during stance phase were investigated using pedobarography. Walking and running trials shared a J-shaped CoP trajectory with greater localization of CoP origin as speed increased. Slight variations of 4th toe position in walking affect CoP origin and modulation of 4th toe pressure on the substrate allows correction of balance, primarily at the beginning of stance phase at lower speeds. Load distribution patterns differed significantly between slow and fast trials. In walking, the 3rd and particularly the 4th toe exhibited notable variation in load distribution with minor claw participation only at push-off. Running trials yielded a distinctly triangular load distribution pattern defined by the 4th toe tip, the proximal part of the 3rd toe and the claw tip, with the sharp point of the claw providing an essential traction element at push-off. Consistency of CoP trajectory and load distribution at higher speeds arises from dynamic stability effects and may also reflect stringent limitations to degrees of freedom in hindlimb joint articulation that contribute to locomotor efficiency. This novel research could aid in the reconstruction of theropod locomotor modes and offers a systemic approach for future avian pedobarographic investigations.

Key words: ostrich, toe function, didactyl, centre of pressure, dynamic pressure distribution.

INTRODUCTION

The ostrich (*Struthio camelus*, Linné 1758) is capable of remarkable speed and exceptional endurance – a rare combination that indicates a high degree of specialization for terrestrial locomotion. In their native Africa, these 150 kg birds range over extensive territories of 25 km^2 and have been filmed running steadily for 30 min at speeds exceeding 60 $km\,h^{-1}$ with step lengths of up to 5 m (e.g. Alexander et al., 1979; Grzimek and Grzimek, 1959; Hallam, 1992). Each day over a 60 year lifespan, up to 8 h are spent walking, grazing and running (Bertram, 1992; Williams et al., 1993).

Ostrich hindlimb morphology provides the mechanical basis for this unique locomotor performance. Within the group of large cursorial ratite species like emu (*Dromaius novaehollandiae*), rhea (*Rhea* spp.) and cassowary (*Casuarius* spp.), ostriches possess the longest limbs, allowing them to achieve great step lengths (e.g. Gatesy and Biewener, 1991; Schaller et al., 2005). The combination of proximally concentrated hindlimb muscle mass and long, light distal leg segments enables high stride frequency under the principles of pendulum dynamics. The lower hindlimb is primarily activated by long tendons that store and release elastic energy during fast locomotion to provide an energetic advantage (e.g. Alexander, 1984). This multi-jointed muscle–tendon system functionally interconnects pelvis and toes, and couples the flexion and extension of joints throughout the hindlimb (Weissengruber et al., 2003). Ligaments at the hip, knee and intertarsal joints direct and constrain mediolateral joint motion, allowing muscle force to be applied predominantly to limb movement through the fore–aft plane (e.g. Firbas and Zweymüller, 1971; Fuss and Gasser, 1992). Specific intertarsal joint ligaments, in combination with joint surface protrusions, passively stabilize the intertarsal joint in an extended position to maintain the columnar support provided by the tibiotarsus/tarsometatarsus to reduce the metabolic cost of trunk support during stance phase (Schaller et al., 2009).

Unique adaptations are also evident in ostrich toe morphology (Fig. 1). While all other birds have three or four toes, the heavy ostrich carries its body mass on only two phalanges: the 3rd major claw-bearing toe and the lateral 4th toe. It is generally assumed that ostrich toe reduction reflects a progressive step in locomotor performance comparable to the evolutionary trend seen in horses (Gangl, 2001; Hallam, 1992). Toe reduction largely eliminates corresponding musculature, thus decreasing distal limb mass and further optimizing swing dynamics. Another ostrich-specific adaptation is evident in the supra-jointed toe posture wherein the metatarsophalangeal joint and proximal phalanx of both toes are permanently elevated above the ground plane as indicated in Fig. 1, upper left and right (Deeming, 2003; Kistner and Reiner, 2002).

Thus, the ostrich stands, walks and runs on the distal phalanges of its toes in contrast to all other birds that are truly digitigrade. The resulting 'additional' limb joint increases the capacity for shock absorption and constitutes an important reservoir for elastic energy storage (e.g. Rubenson et al., 2007; Schaller et al., 2005). Textured fat pads envelop and protect the bones of both toes, conform to the

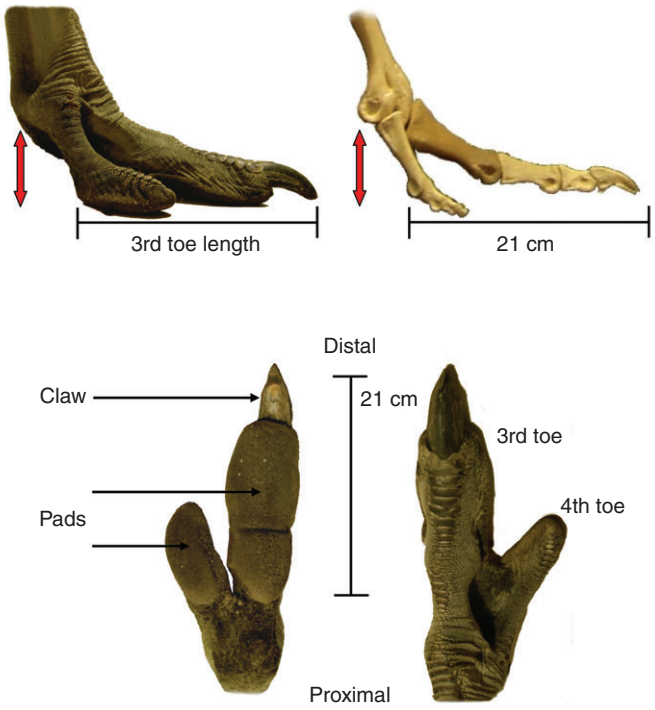

Fig. 1. Right phalanges of an adult ostrich (anatomical specimen). Clockwise from top left: lateral view of anatomical specimen, skeleton, dorsal view, ventral view. Red arrows indicate elevated metatarsophalangeal joint.

substrate and provide additional stress absorption upon ground contact (Fig. 1, lower left).

Despite comprehensive kinematic analyses of ostrich locomotion (e.g. Abourachid and Renous, 2000; Gatesy and Biewener, 1991; Rubenson et al., 2004), previous studies have not included detailed examination of the interaction between toes and substrate. The only surveys regarding phalangeal function are ichnotaxonomic analyses comparing ostrich and emu toe prints with fossilized trackways to aid in the reconstruction of theropod gait patterns (Farlow, 1989; Milán, 2006; Padian and Olson, 1989). Although a valid palaeontological approach, toe print analysis delivers a static depth profile without capturing the roll-off sequence through stance phase.

In this study we explored ostrich toe function *in vivo* to determine the specific role played by the toes in providing support, grip and balance in this fast, heavy, endurance runner. Phalangeal roll-off patterns during voluntary overground walking and running were assessed based on spatio-temporal pressure distribution data and centre of pressure (CoP) trajectories. This real-time pedobarographic technique quantifies the relative load-bearing capacities of the major claw-bearing 3rd toe and laterally oriented 4th toe and allows detailed analysis of 4th toe function in the maintenance of balance. To our knowledge, this is the first analysis of phalangeal dynamic pressure distribution in any avian species. Thus, a secondary goal of this study was to establish a system of data acquisition and assessment applicable to future studies on avian terrestrial locomotion.

Because of proposed similarities in behaviour and habitat, the bipedal ostrich is a valuable model for the theoretical reconstruction of locomotor modes in theropod dinosaurs (Farlow et al., 2000; Gatesy, 1991). We hope these results contribute to this inquiry and perhaps add to the debate about toe reduction in avian species over the course of evolution.

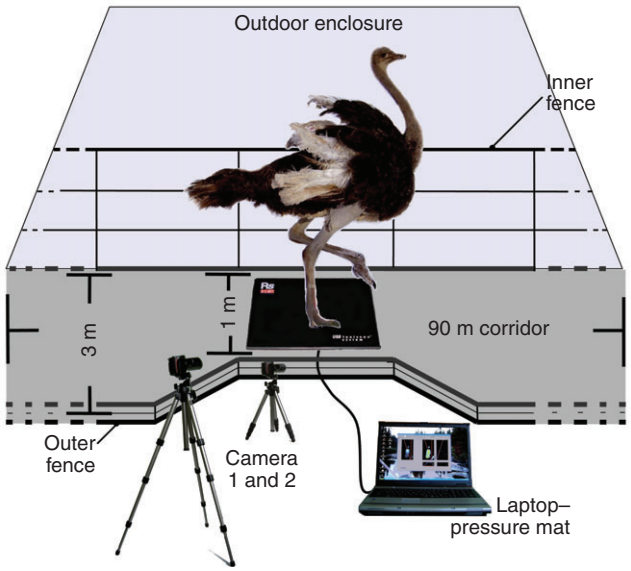

Fig. 2. Schematic diagram of the on-site data acquisition system.

MATERIALS AND METHODS

Test specimens

Five genetically unrelated ostrich chicks (*Struthio camelus australis*) were hand-raised from the age of 10 weeks to foster acceptance of human contact and allow them to become familiar with the experimental set-up. The most co-operative specimens – two full-grown females, 3 years old and ~90 kg – were selected as subjects for this study. All ostriches are kept year-round in an outdoor enclosure of grassland (6400 m) near Heidelberg, Germany. The birds had *ad lib*. access to water, pasturage and ostrich fodder with seasonally dependent composition. Living conditions were in accordance with the official guidelines for ostrich keeping as regulated by German law. The specimens were not subjected to surgery or any form of invasive physical manipulation and were in excellent physical condition with a properly elevated metatarsophalangeal joint, representing average body proportions and mass for birds of their age and sex (Deeming, 2003).

Set-up and data analysis

A 90 m long×3 m wide fenced-in corridor was separated from the main enclosure by a 2 m tall wire mesh which narrowed to 1 m wide over a length of 3 m where the data acquisition system was located (Fig. 2). The set-up consisted of one RSscan International® pressure plate (45×30 cm, 250 Hz sampling and 16,384 pressure sensors of 0.375 cm^2, USBII interface; Ipswich, UK) placed on the ground to record dynamic pressure distribution. The rigid pressure plate was contained within a specially designed support frame constructed from a 13 mm polycarbonate sheet to ensure a solid flat surface and stable plate position. The plate was covered with a 2.5 mm non-slip rubber sheet to prevent possible damage from the claw. The encased pressure plate was placed upon damp packed sand and level conditions were confirmed at 10 min intervals using a spirit level. Data acquisition and subsequent data processing were carried out using Footscan MST software 6.2 and 6.3 (RSscan International®). One digital camera (Canon MV 900;

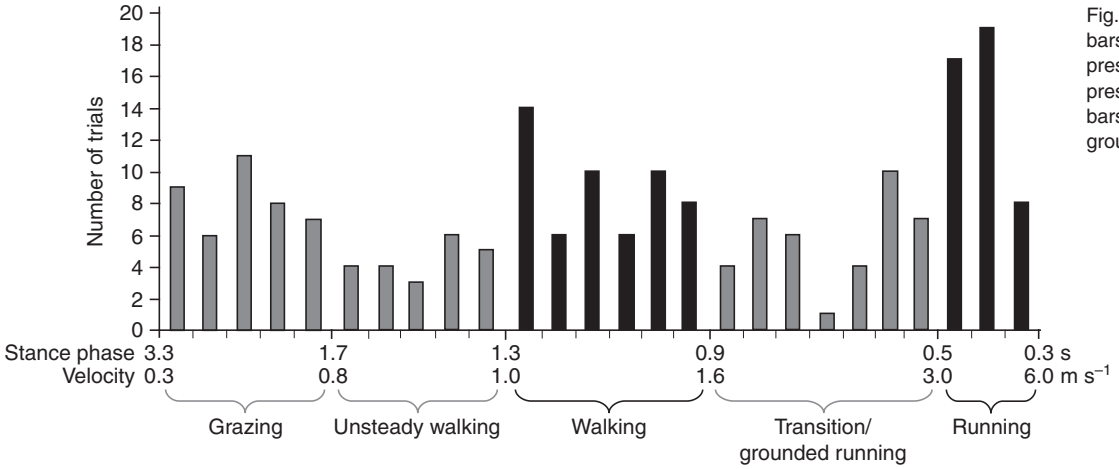

Fig. 3. Gait classification. Black bars indicate the 98 trials used for pressure distribution and centre of pressure (CoP) analysis; grey bars indicate unsteady and grounded running trials.

50 frames s^{-1}) was located 3 m from the corridor fence and recorded overall body posture and stride patterns. A second camera (Canon MV 550i; 50 frames s^{-1}), synchronized with camera 1, recorded close-up detail of the phalanges during ground contact. Cameras were perpendicular to the sagittal plane of motion. Ostriches performed voluntarily without physical manipulation, ensuring that data reflected a natural stride cycle. When necessary, locomotion was initiated either by display of food at the end of the corridor or by the lead scientist moving ahead to compel the ostrich to follow.

Over 400 trials were recorded over a 3 day period of clement summer weather. Of these, a total of 200 trials with complete footfalls were obtained and collated to assess the relationship of stance phase duration to speed (Fig. 3). Speed was estimated on the basis of the lateral full-body video images relative to visual markers installed at 1 m increments on the corridor fence, wherein movement of a marker at the sternum of the ostrich relative to fence markers was analysed using digitized video frames (Didge, Alistair Cullum, Creighton University, Omaha, NE, USA). Video footage also provided qualitative information that allowed classification of a particular trial within a specific locomotor category subsequently divided into grazing, unsteady and steady walking, acceleration/deceleration, grounded running and running with an aerial phase. Finally, the relationship between stance phase duration and velocity for each of the 200 trials was determined by synchronizing a trial's pressure plate data with its corresponding video footage. The results of this analysis are plotted in Fig. 3.

To ensure a reliable baseline for pedobarographic assessment of walking and running gaits, only trials featuring ostriches moving in a steady forward direction with synchronous swing phases were considered valid for phalangeal pressure and CoP trajectory analysis. Trials with velocities in the range 1.0–1.6 m s^{-1} with stance phase durations of 1.3–0.9 s and duty factor above 0.5 were identified as walking gaits. Trials were identified as running gaits when duty factor was below 0.5 and velocity was between 3 and 6 m s^{-1}, with stance phase durations of 0.5–0.3 s. Of the 200 trials, 98 were steady gaits; of these, 54 were walking trials and 44 were running trials (shown as black bars in Fig. 3).

Unsteady gaits were identified as such when asynchronous swing phases were observed with unequal step lengths/stance phases over two stride cycles. These occurred during grazing and uneven walking, and at higher velocities between 1.6 and 2.5 m s^{-1}. This specific speed range, with birds either accelerating or decelerating, indicated a transition between walking and running gaits. At speeds from 2.5 to 3.05 m s^{-1} ostriches employ a grounded running gait with duty factor >0.5 (Rubenson, 2005; Rubenson et al., 2004). As our primary interest was to identify clear differences in phalangeal pressure distribution during walking and running, trials of intermediate-speed grounded running were also disregarded in pedobarographic analysis. For completeness, all unsteady trials and transitions from walking to running, including grounded running trials, are shown as grey bars in Fig. 3.

The CoP trajectory was calculated as a function of time. Pressure measurements are indicated in arbitrary units (a.u.) to quantify the relative participation of phalangeal elements (1 a.u.≈1 N per sensor). Three distinct toe regions were defined: (1) the 3rd toe, (2) the claw tip and (3) the 4th toe (Fig. 4). For each toe region, the mean pressure was plotted as a function of time, which was normalized against the total ground contact duration of all elements. Additional data were derived from the toe pressure profiles including: (1) total ground contact area, (2) individual ground contact area for 3rd toe, 4th toe and claw, (3) functional 3rd toe length, i.e. the distance

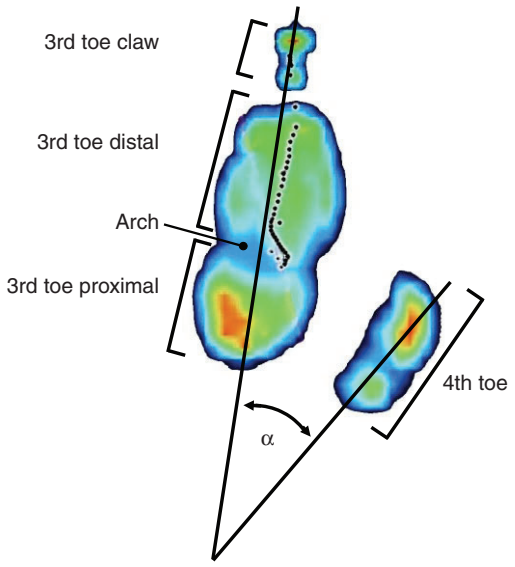

Fig. 4. Footscan image of a typical running trial. Loads are indicated on a gradient from red (very high) to dark blue (very low). Partially dotted line illustrates CoP path (dot interspace, 4 ms). α, angle between long axis of 3rd and 4th toe.

between the most proximal part of the ground contact area (second phalanx) and the tip of the claw, and (4) degree of 4th toe abduction (Fig. 4). In order to explore the potential for inter-individual variation, peak pressure values of walking and running trials from each specimen were subjected to an analysis of variance (ANOVA). A total of 98 samples (specimen one, 53 samples; specimen two, 45 samples), equally divided between walking and running speeds, were included in this statistical analysis.

Manual manipulation and foam track capture of ostrich toe prints

Three fresh, intact anatomical specimens (adult male and female ostriches, 90–105 kg) of the lower hindlimb (severed at the intertarsal joint) were manipulated prior to the onset of rigor mortis to determine 4th toe articulation range. The 3rd toe was held immobile on a flat surface in a 'standing' position with the 4th toe overhanging the edge of the flat surface, thus allowing the 4th toe to be manually induced to the limit of its motion range in all directions. The excursion distance of the 4th toe tip from nominal position and angle relative to the main axis of the third toe were noted. Maximum mediolateral 4th toe motion range was also recorded using orthopaedic foam for reference. When exposed to pressure, this industry-standard semi-rigid foam retains the exact shape of the distorting element to preserve a highly detailed impression. Toe prints of anatomical specimens were obtained by manually exerting pressure on the proximal part of the limb in a downward vertical direction into the foam surface to establish the default 4th toe position, and then repeated with the 4th toe held in the maximal mediolateral excursion position as noted above. To provide cross-reference to *in vivo* toe position, foam toe print capture of walking and running gaits was undertaken with our live ostriches in the outdoor enclosure.

RESULTS

Dynamic pressure distribution in walking and running

In walking trials, mean peak integrated pressure of the combined ground contact elements occurred at 67% of stance phase. Generally, the 4th toe attained maximum loading after 30% of stance phase while load increased simultaneously at the proximal and distal portion of the 3rd toe, shifting to the distal area of the 3rd toe, reaching maximum load at 70% of stance phase (Figs 5 and 6). While 3rd toe pressure values followed a consistent pressure distribution pattern, the participation of the smaller 4th toe seemed relatively unpredictable. This observation is reinforced by the much higher standard deviation seen in 4th toe pressure data when compared with those of the 3rd toe once standard deviation values are normalized in accordance with the 1:3 ratio of contact surface area. In extreme trials, the 4th toe bore a low of 3% and a high of 50% of the entire load within the first 15% of stance phase. While the 3rd toe typically supported the majority of the load (93% at peak; Table 1), occasional high load bearing in the 4th toe resulted in relatively lower load bearing in the 3rd toe. With the exception of

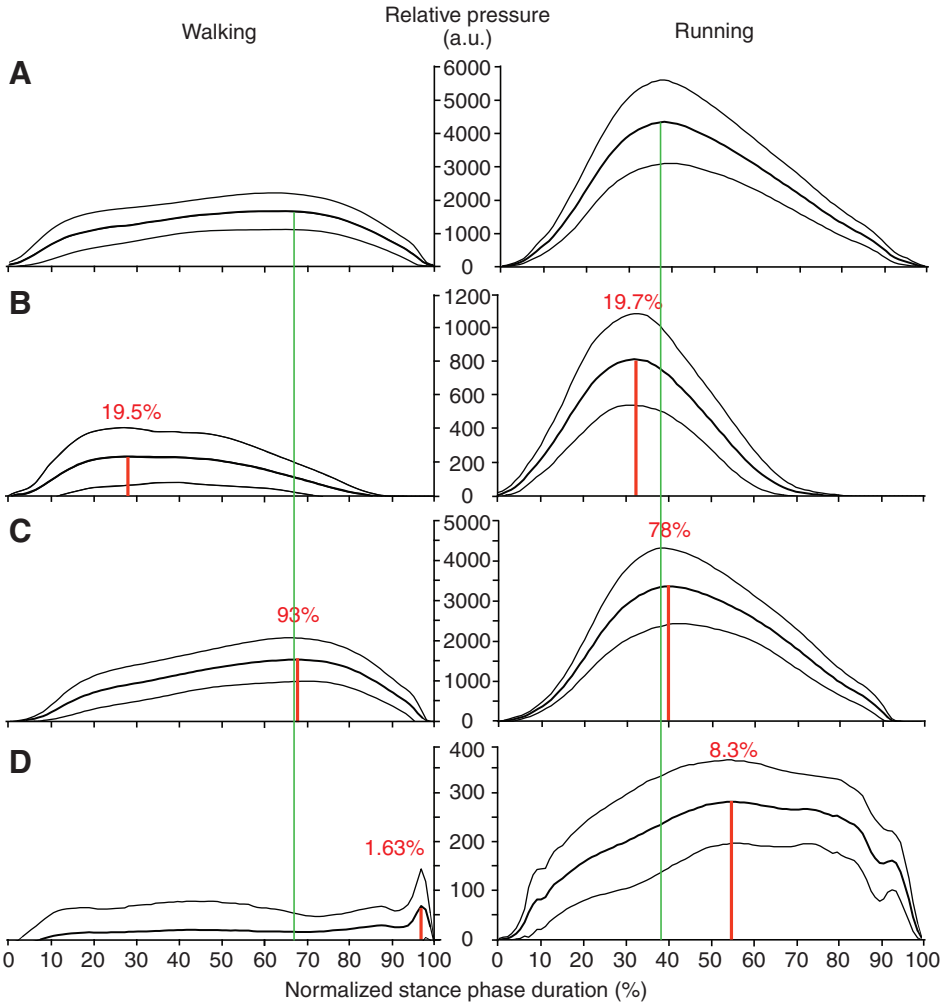

Fig. 5. Load distribution in walking and running trials. Pooled data from 54 walking trials and 44 running trials showing an integrated pressure curve for all phalangeal elements (A) and pressure curves for each phalangeal element in isolation (B, 4th toe; C, 3rd toe; D, claw). Mean load (bold black line) and s.d. (thin black lines) are shown. Green lines indicate the moment of integrated peak pressure; red lines indicate the moment of peak pressure for each ground contact element. The percentage of total load at peak load bearing for each element is given above the curves.

Table 1. Pooled data-set for surface areas, and peak loads and standard deviation

		Load (%)		s.d. (%)	
	Surface area (cm^2)	Walking	Running	Walking	Running
Total	80.7±1.00	100.0	100.0	34	28
4th toe	19.1±0.25	19.5	19.7	70	35
3rd toe	57.5±0.50	93.0	78.0	37	26
Claw	4.1±0.25	1.6	8.3	32	29

3rd toe length in the two ostrich specimens from claw tip to proximal 3rd toe end amounted to 19.6±1 cm.
Data are mean load bearing at peak pressure over time and standard deviation from mean peak pressure.

toe-off, the claw bore negligible pressure and was essentially uninvolved in walking (Fig. 5).

In running trials, the dynamic pressure distribution showed a different contour from the curve seen in walking, with a rather sharp peak at 40% of stance phase and very short, simultaneous peak times for the 3rd and 4th toe (Fig. 5). As in walking trials, 3rd toe peak pressure was substantial at 78% of total phalangeal load bearing. Particularly high loads were recorded for the proximal segment of the 3rd toe, the tip of the 4th toe and the claw, resulting in a tripod-like pattern of ground contact elements evident throughout all running trials (Fig. 6).

During running, lower load was evident at the distal 3rd and proximal 4th toe when compared with walking. With load decreased on the distal 3rd toe, a concurrent increase of load appeared at the claw, possibly to ensure that the claw tip is firmly embedded in the ground at higher speeds. This was confirmed by the significantly higher load values of the claw which, when compared with walking, showed that the claw sustained load throughout the entire stance phase (Figs 5 and 6).

In summary, absolute load values were substantially higher in running because of the inherently greater ground reaction forces resulting from the shorter stance phase duration available to generate the vertical impulse (force–time integral) at higher speeds. Hence, the integrated load maxima of the 3rd and 4th toe in running occurred within a much smaller time frame in both absolute and relative terms. In both walking and running, the 4th toe reached peak pressure values first, followed by the 3rd toe and finally the claw. As 3rd toe peak pressure was the highest out of all phalangeal elements at all speeds, it largely influenced the timing of integrated peak pressure. As the speed of the ostriches increased and duty factor decreased, the curve of integrated peak pressure seen in the second third of stance phase in walking appeared more spiked in running, with the peak shifted towards the first third of stance phase (Fig. 5). When comparing load distribution data of the two specimens at similar speeds, statistical analysis of 98 samples showed that there was no significant inter-individual variation in either walking or running trials.

CoP path in walking and running

In walking, the CoP path traversed a larger area and was generally less consistent than in running. This arose from the wide spatial distribution of CoP origin during the initial 15% of stance phase, with CoP originating within an area 7 times larger than that seen in running trials. At 70% of stance phase, CoP was located close

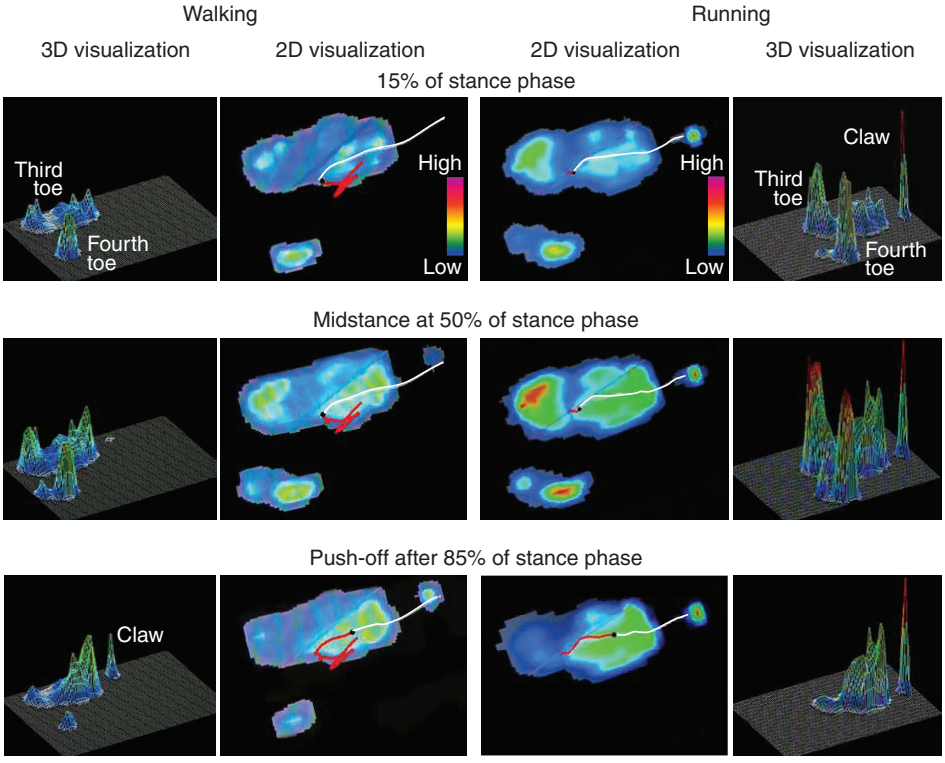

Fig. 6. Sequence of dynamic pressure distribution in a typical walking and running trial. The red/white line maps the trajectory of CoP over the duration of the sample, where red represents the completed CoP path and white represents the CoP path trajectory following the time point of the sample indicated by the black dot. Loads are indicated on a gradient from red (very high load) to dark blue (very low load).

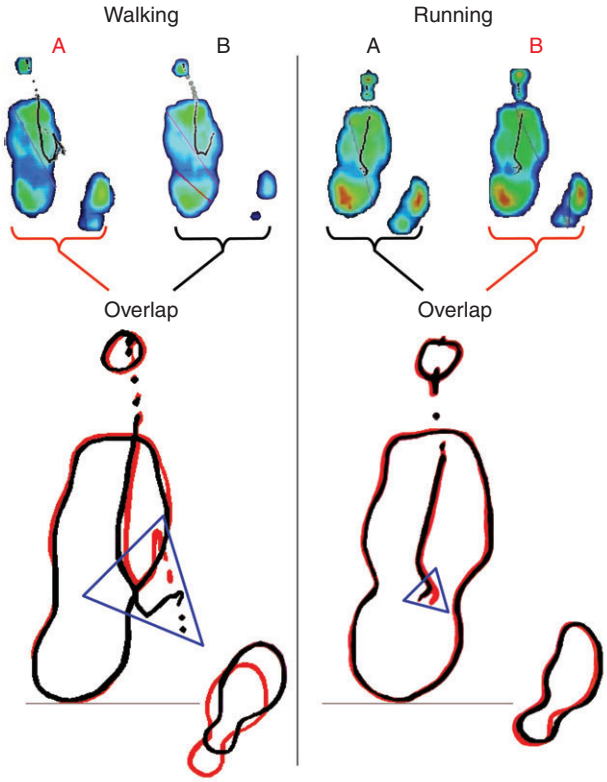

Fig. 7. Comparison of CoP origin and 4th toe position in walking and running trials. Blue triangle shows area of CoP origin from 16 walking trials and 16 running trials sampled equally from the two subjects (A and B). CoP in walking originated in an area 7 times larger than that in running.

to the lateral edge/arch of the 3rd toe, and finally travelled anterograde, resolving with a rapid push through the claw tip (Fig. 6). Generally, CoP never originated medial to the longitudinal axis of the 3rd toe and never in the proximal part of the 3rd toe. There was close correlation between decreased speed and increased divergence of CoP origin in walking (Fig. 7).

CoP origin during running consistently fell within a defined area located within, or just lateral to, the arch of the 3rd toe (Fig. 6). Within the first 15% of stance phase, CoP moved to the longitudinal centre of the distal 3rd toe where it remained for ~70% of stance phase. Thereafter, CoP continued in an anterograde direction and, at push-off, resolved at the tip of the claw. When comparing walking and running trials through graphical overlapping as in Fig. 7, variations in 4th toe position could be linked to velocity – as speed decreased, mediolateral and craniocaudal variation increased.

4th toe motion range

Manual manipulation experiments with fresh anatomical specimens showed that the 4th toe has a wide range of motion in the dorsoventral plane. With the 3rd toe fixed in position, the maximum dorsoventral motion range of the 4th toe was 11 cm (red line in Fig. 8), and mediolateral excursion amounted to 4.5 cm (blue line in Fig. 8) with a maximum angle of 34 deg between the 3rd and 4th toe main axes. Maximum craniocaudal motion range was 2 cm (black line in Fig. 8) with angles from 22 to 34 deg relative to the 3rd toe (Fig. 9B). When manually extending the 3rd toe, the 4th toe automatically abducted to a default angle of 28 deg (Fig. 9A). This coupled toe motion is regulated by an interphalangeal ligament inserting mediodistally at the proximal phalanx of the 3rd toe and

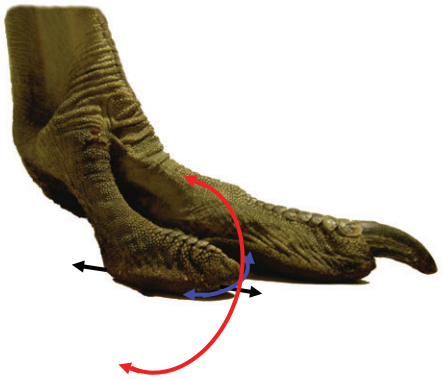

Fig. 8. 3D motion range of the 4th toe in a fresh anatomical specimen. Red line shows maximum dorsoventral motion range of the 4th toe (11 cm), blue line shows maximum mediolateral excursion (4.5 cm), black line shows maximum craniocaudal motion range (2 cm).

medioproximally at the second phalanx of the 4th toe. This ligament, shown in Fig. 9C, also limits maximum toe abduction to 34 deg relative to the 3rd toe main axis (Schaller, 2008).

The maximum mediolateral and craniocaudal motion range of anatomical specimens was identical to the motion range obtained from *in vivo* pressure plate measurements and pressure foam imprints collected from our live specimens.

DISCUSSION

This study presents the first pedobarographic analysis of overground walking and running ostriches. The large number of trials yielded reliable data on dynamic pressure distribution and CoP trajectory, allowing interpretation of toe function in this flightless, cursorial bird. Having selected two genetically unrelated subjects of the same sex and similar age and size, the consistency of inter-individual results in running trials accurately document a generalized pattern in ostrich locomotion.

This general pattern was evident in CoP trajectories once CoP had reached the arch of the 3rd toe after the first 15% of stance phase. In both walking and running, CoP followed a consistent, strictly anterograde path. Additional analyses of unsteady walking, acceleration/deceleration and grounded running trials also reflected this pattern. A morphological explanation for this consistency may be found in the passive locomotor apparatus, which interacts with the multi-jointed muscle–tendon system. Herein, ligaments largely guide and constrain the range of mediolateral joint movement to concentrate muscle power for the activation of the limb in the fore–aft plane (Fuss and Gasser, 1992; Schaller, 2008; Weissengruber et al., 2003). Previous research has also shown that the distal limb is passively stabilized by ligaments at the extended intertarsal joint during stance phase (Schaller et al., 2009). This engage–disengage mechanism (EDM) tunes limb stiffness through a load-based feedback loop that acts at the intertarsal (ankle) joint to provide columnar support for the trunk. Taken as a whole, it appears that leg anatomy is largely responsible for the highly consistent CoP path seen after the phalanges have established stable ground contact.

The greater standard deviation for load distribution data in walking compared with running is not unexpected (Table 1). During slow walking in particular, the maintenance of stability requires a greater degree of nervous and muscular control of ground contact elements

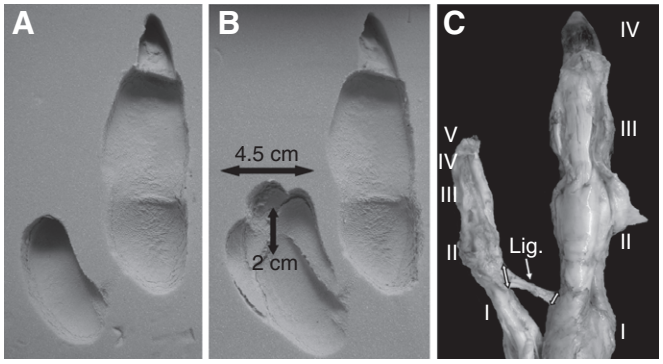

Fig. 9. 2D motion range of the 4th toe in a fresh anatomical specimen and dissected phalanges. (A) Imprint of default position created by left toes in orthopaedic pressure-sensitive styrofoam; (B) maximum motion range of 4th toe medially and laterally of default imprint; (C) dissected right phalanges of adult ostrich (ventral view, musculature removed) with interphalangeal ligament (lig.) preventing over-abduction of the 4th toe. Roman numerals indicate each phalanx of the 3rd and 4th toe.

than during running, when dynamic stability aids balance (e.g. Kummer, 1959). This is reflected in the load distribution of individual ground contact elements in running trials, where maximum pressure is concentrated closer to the moment of integrated peak pressure (Fig. 5, red lines relative to green line), indicating that the 3rd toe, its claw and the 4th toe function more as a single entity at higher speeds (3–6 m s^{-1}). It is expected that, as speed increases, standard deviation would decrease and reach very low values during top-speed running. Indeed, analysis of only the fastest running trials in our study (5–6 m s^{-1}) resulted in a standard deviation of only 19% compared with pooled running standard deviation values of 28%. This trend is understandable when considering the little time available for positional compensation of phalangeal elements when running at 16.67 m s^{-1} (60 km h^{-1}) at a duty factor of 0.29 when stance phase is very short (Alexander et al., 1979).

Investigation of top running speeds is a priority for future experiments. This will certainly require a more extensive set-up allowing the birds a longer corridor for data gathering. It would also be interesting to collect pressure data of left and right phalanges for a more detailed analysis of a complete stride cycle. Ultimately, a conclusive investigation should also incorporate turning and cutting manoeuvres.

4th toe functions as an outrigger

The maintenance of balance from stride to stride requires articular compensation within the limb and compensation at ground level *via* phalangeal elements. The latter is especially important in the long-limbed ostrich with a centre of mass (CoM) at 1–1.3 m above ground, where compensatory functions at ground level appear to be provided by the 4th toe. The 3rd toe and its claw – essentially forming an elongation of the tarsometatarsal main limb axis – absorb most of the high stress at touch-down and ensure reliable load bearing and grip during stance phase. Strong ligaments, the fascia and shock-absorbing fat pads envelop the toe skeleton and interphalangeal joints to ensure structural integrity but consequently limit 3rd toe mobility.

The lateral 4th toe, in contrast, provides a degree of fine adjustment through its inherently greater 3D motion range. This presumably allows compensation for uneven ground conditions to correct potential imbalances in CoM, particularly at slower speeds (e.g. Hof, 2008). This is illustrated in the consequential relationship of 4th toe position to load distribution and CoP, and probably explains the wider variability of CoP origin in walking.

In addition, 4th toe peak load in walking occurs at the beginning of stance phase when balance adjustments are critical to establish stability for the later stages of stance phase. This ‘outrigger’ hypothesis gains further weight when assessing the standard deviation of the 3rd and 4th toe separately. Here, the standard deviation of the rather constrained 3rd toe is low at all speeds, while the standard deviation for the 4th toe is as high as 70% in walking compared with 35% in running (Fig. 5). The significantly lower variation in load distribution when running illustrates the effects of dynamic stability, which reduces the demand for fine adjustment at the 4th toe. However, as in walking, the smaller toe is still subjected to a mean of 20% of overall load with a pronounced area of peak pressure at the toe tip forming one corner of the typical tripod-like load distribution pattern. The above points, taken as a whole, serve to establish the important role of the 4th toe in the maintenance of balance.

Discussions about further reduction and eventual elimination of the 4th toe arise from the perspective that evolutionary imperatives dictate a gradual discarding of structures and functions that are deemed biologically redundant. Although the reduction from three toes to two in the ostrich certainly appears to reflect an evolutionary progression, possible 4th toe reduction must be considered within the context of the ostrich as a biped. Phalangeal reduction in the quadrupedal horse was possible because body mass is carried on four limbs with a consequently large base of support (e.g. Hof, 2008; Kummer, 1959). In the bipedal ostrich, the 4th toe provides a significant increase in the base of support because of its lateral orientation, resulting in the typical triangular pressure profile.

As a further note of interest on the topic of toe reduction, static depth profiles of the phalanges of running emus showed that, as speed increases, the 2nd toe bears proportionately less load. This was shown by the relatively shallow 2nd toe imprints from running samples compared with a deeper profile seen in walking toe prints (Milán, 2006). It is this medial toe – common to all ratites – that has been completely reduced in the ostrich. Further exploration of emu toe function may indicate a possible evolutionary route towards didactylism in this group of birds.

Claw as positional anchor during running

In walking trials, the claw exerted only minor pressure throughout stance phase except for an incidental peak at toe-off registering 1.6% of total phalangeal load. At running speeds, the claw exerted 5 times the amount of pressure seen in walking, with the claw tip subjected to 8% of the total load. This force is concentrated on a surface area of only 4 cm^2 and renders peak pressures of 40 kg cm^{-2}. This was clearly illustrated in the toe prints of our ostriches after walking or running over damp sand. Predictably, the imprint of the claw was much more pronounced when running because of the greater ground reaction forces present at higher speeds (N.U.S. and R.V., unpublished observations).

However, it also appears that deeper substrate penetration by the claw at higher speeds is driven to some degree by an anatomical precondition. We performed an additional experiment with an isolated lower ostrich limb (intact tarsometatarsus and phalanges) wherein the toes were placed on a flat surface with the tarsometatarsus oriented vertically as in a standing ostrich. Variable pressure was applied manually from above through the long axis of the tarsometatarsus to observe changes in phalangeal position. With little or no pressure exerted, the claw tip remained

slightly elevated and did not contact the substrate. This is reflected in our findings for walking ostriches, where claw participation during stance phase was minor or absent as indicated by low load-bearing values. When the limb was subjected to an energetic downward thrust, the claw of the dissected limb instantly moved into a more pronounced downward-facing position and contacted the substrate with a force loosely scaled to the power of the manual thrust. This automated reaction would have greater consequence given the forces generated by a running ostrich, especially considering the interaction of toe flexors and extensors within the multi-jointed muscle–tendon system during stance phase (Weissengruber et al., 2003).

A visual assessment of the claw's shape suggests its crucial function in ostrich locomotion (Fig. 8). The claws can grow to lengths between 5 and 10 cm (N.U.S., unpublished data); a coronal plane cross-section renders a triangular shape with its leading point oriented cranially. In the lateral view, the downward curving claw is undercut at a 45 deg angle to form a sharp point at its distal end. This profile permits reliable resistance to dislocation once embedded in the ground by providing a straight segment of the triangle perpendicular to the vector of force application during propulsion. Considering that the pads of the plantar surfaces would not provide sufficient traction at speeds of 16 m s^{-1} – especially on granular or slippery substrates – the claw provides a solid positional anchor and a final lever to maximize energy transfer at push-off.

Perspectives

In future applications, pedobarographic equipment could be employed in comparative studies of the emu, cassowary and rhea to examine toe function in these related extant cursorial avian species. In particular, it would be interesting to determine the differences – or similarities – in load distribution patterns between a didactyl bird with an elevated metatarsophalangeal joint and three-toed flightless birds with grounded metatarsophalangeal joints. An inclusive data set of ratite dynamic pressure data in combination with static trackway analyses could contribute to projections of theropod locomotion. This may include hypotheses relating to the anatomy of ground contact elements, CoP trajectories and limb dynamics and could refine reconstruction of theropod gait patterns and estimates of velocity, which, at this point, are largely based on step and leg lengths and projected leg postures.

CONCLUSIONS

The area of CoP origin is more dispersed in walking than in running presumably because of the lack of dynamic stabilization effects at slower speeds. Variation in CoP origin results from the greater requirement for fine adjustment of 4th toe position and degree of flexion to manage load and CoM in response to ground conditions and overall body posture at walking speeds. However, there is little divergence from a predictable CoP path and its relative duration at both walking and running speeds once the toes are firmly positioned on the substrate. This consistency is probably dictated by morphological constraints to lateral degrees of freedom that stabilize the entire leg during the last phase of ground contact.

The single remaining claw, as the only rigid element of the toes, functions as a positional anchor at higher velocities once embedded in the substrate. Despite consideration of a possible evolutionary reduction of the 4th toe, its important role as an outrigger for balance in walking and as a significant load-bearing element at all speeds render this outcome highly unlikely.

ACKNOWLEDGEMENTS

Special thanks are due to Dr O. Faulhaber for his professional practical assistance during data gathering, J. Gass for his continuing ostrichophile caretaking, the Centre for Research and Conservation of the Royal Zoological Society of Antwerp (Belgium) for providing us with the pressure plate and accessories, Straussenfarm Donaumoos (Leipheim, Germany) for providing samples for morphological study, and the CUSANUSWERK Foundation (Bonn, Germany) for their financial support.

REFERENCES

Abourachid, A. and Renous, S. (2000). Bipedal locomotion in ratites (Palaeognatiform): examples of cursorial birds. *Ibis* **142**, 538-549.
Alexander, R. (1984). Elastic energy stores in running vertebrates. *Am. Zool.* **24**, 85-94.
Alexander, R., Maloiy, G. M. O., Njau, R. and Jayes, A. S. (1979). Mechanics of running in the ostrich (*Struthio camelus*). *J. Zool. (Lond.)* **187**, 169-178.
Bertram, B. C. R. (1992). *The Ostrich Communal Nesting System*. Princeton, NJ: Princeton University Press.
Deeming, D. C. (2003). *The Ostrich – Biology, Production and Health*. Cambridge: Cambridge University Press.
Farlow, J. O. (1989). Ostrich footsprints and trackways: implications for dinosaur ichnology. In *Dinosaur Tracks and Traces* (ed. D. D. Gillette and M. G. Lockley), pp. 243-248. New York: Cambridge Uniiversity Press.
Farlow, J. O., Gatesy, S. M., Holtz, T. R., Jr, Hutchinson, J. R. and Robinson, J. M. (2000). Theropod locomotion. *Am. Zool.* **40**, 640-663.
Firbas, W. and Zweymüller, K. (1971). Über das Hüftgelenk der Ratiten. *Gegenbaurs Morph. Jahrb.* **116**, 91-103.
Fuss, F. K. and Gasser, C. R. (1992). Cruciate ligaments of the avian knee: insight into a complex system. *J. Morphol.* **214**, 139-151.
Gangl, D. (2001). Die Muskeln der Hinterexremität des Strausses (*Struthio camelus* Linné 1758). Inaugural-Dissertation, Veterinärmedizinische Universität Wien, 151pp.
Gatesy, S. M. (1991). Hind limb scaling in birds and other theropods: implications for terrestrial locomotion. *J. Morphol.* **209**, 83-96.
Gatesy, S. M. and Biewener, A. A. (1991). Bipedal locomotion: effects of speed, size and limb posture in birds and humans. *J. Zool.* **224**, 127-147.
Grzimek, B. and Grzimek, C. (1959). *Serengeti Shall Not Die*. West Germany: Asta Motion Pictures.
Hallam, M. G. (1992). *The Topaz Introduction to Practical Ostrich Farming*. Harare, Zimbabwe: The Ostrich Producers' Association of Zimbabwe.
Hof, A. L. (2008). Mechanics of balance. In *Advances in Plantar Pressure Measurements in Clinical and Scientific Research* (ed. K. D'Août, K. Lescrenier, B. Van Gheluwe and D. DeClercq), pp. 1-25. Aachen, Germany: Shaker Publishing.
Kistner, C. and Reiner, G. (2002). *Strauße – Zucht, Haltung und Vermarktung*. Stuttgart: Eugen Ulmer Verlag.
Kummer, B. (1959). *Bauprinzipien des Säugerskeletts*. Stuttgart: Georg-Thieme Verlag.
Milán, J. (2006). Variations in the morphology of Emu (*Dromaius novaehollandiae*) tracks reflecting differences in walking pattern and substrate consistency: Ichnotaxonomic implications. *Paleontology* **49**, 405-420.
Padian, K. and Olsen, P. E. (1989). Ratite footprints and the stance and gait of mesozoic theropods. In *Dinosaur Tracks and Traces* (ed. D. D. Gillette and M. G. Lockley), pp. 231-241. New York: Cambridge University Press.
Rubenson, J. (2005). Mechanical energetics as a determinant of the metabolic cost of bipedal locomotion. PhD thesis, University of Western Australia, Perth, Australia.
Rubenson, J., Heliams, D. B., Lloyd, D. G. and Fournier, P. A. (2004). Gait selection in the ostrich: mechanical and metabolic characteristics of walking and running with and without an aerial phase. *Proc. R. Soc. Lond. B* **271**, 1091-1099.
Rubenson, J., Lloyd, D. G., Besier, T. F., Heliams, D. B. and Fournier, P. A. (2007). Running in ostriches (*Struthio camelus*): three-dimensional joint axes alignment and joint kinematics. *J. Exp. Biol.* **210**, 2548-2562.
Schaller, N. U. (2008). Structural attributes contributing to locomotor performance in the ostrich (*Struthio camelus*). PhD thesis, University of Heidelberg, Heidelberg, Germany.
Schaller, N. U., Herkner, B. and Prinzinger, R. (2005). Locomotor characteristics of the ostrich (*Struthio camelus*) – I: morphometric and morphological analyses. In *Proceedings of the 3rd International Ratite Science Symposium of the World's Poultry Science Association (WPSA) and 12th World Ostrich Congress, Madrid, Spain, 14th–16th October 2005* (ed. E. Carbajo), pp. 83-90. Wallingford, Oxfordshire, UK: CABI Publishing.
Schaller, N. U., Herkner, B., Villa, R. and Aerts, P. (2009). The intertarsal joint of the ostrich (*Struthio camelus*): anatomical examination and function of passive structures in locomotion. *J. Anat.* **214**, 830-847.
Weissengruber, G. E., Forstenpointner, G. and Gangl, D. (2003). Gut zu Fuß – funktionell-anatomische Aspekte des bipeden Laufens beim Afrikanischen Strauß (*Struthio camelus* Linné, 1758). *Vet. Med. Austria/Wien. Tierärztl. Mschr.* **90**, 67-78.
Williams, J. B., Siegfried, W. R., Milton, S. J., Adams, N. J., Dean, W. R. J., Du Plessis, M. A., Jackson, S. and Nagy, K. A. (1993). Field metabolism, water requirements, and foraging behaviour of wild ostriches in the Namib. *Ecology* **74**, 390-404.